RSC Applied Polymers

ROYAL SOCIETY OF CHEMISTRY

PAPER

View Article Online
View Journal | View Issue

Cite this: *RSC Appl. Polym.*, 2025, **3**, 438

Assessing the properties of protein foams as an alternative absorbent core layer in disposable sanitary pads†

Athanasios Latras, ‡[a] Mercedes A. Bettelli, ‡[a] Pamela F. M. Pereira, [b] Amparo Jiménez-Quero, [b] Mikael S. Hedenqvist [a] and Antonio J. Capezza *[a]

Developing biodegradable menstrual products using co-stream proteins as a material alternative to fossil counterparts presents a significant environmental advantage across their entire value chain. The intrinsic properties of wheat gluten foams derived from wheat starch production have been validated with respect to their potential as absorbent core layers in disposable sanitary pads, which is relevant to the rising demand for eco-friendly disposable sanitary pad alternatives. Here, we report the fabrication of a gluten-porous absorbent layer and evaluate its liquid absorption properties and mechanical stability under relevant operating conditions compared to a commercial absorbent foam layer used in sanitary pads. The porosity was achieved using sodium and ammonium bicarbonate, which are non-toxic and food-grade blowing agents, and the materials were shaped/foamed using a conventional oven. The use of sodium bicarbonate resulted in a more homogeneous and lower-density foam with smaller pores than with ammonium bicarbonate. The developed prototypes show comparable mechanical properties under compression to foams used in commercial pads, retaining up to 95% of their initial shape after 3 h of compression. Moreover, the foamed structure permitted a liquid uptake of saline and blood of 4.5 g g^{-1} and 1 g g^{-1}, respectively, with the possibility to absorb up to 1.5 g g^{-1} of saline under load. The results indicate that the choice of blowing agent has a large impact on the performance of gluten pads under constant pressure. It is thereby demonstrated here that protein-based foams have adequate mechanical and absorption properties that make them interesting for their future use as the absorbent layer in sanitary products following a circular economy model.

Received 24th October 2024,
Accepted 5th February 2025

DOI: 10.1039/d4lp00323c

rsc.li/rscapplpolym

1. Introduction

With the environmental regulations becoming more stringent, there is a need to shift from fossil-based to bio-based plastics and from landfill waste accumulation to materials that biodegrade. This is needed since waste accumulation and microplastic generation are increasing, especially within personal hygiene and sanitary single-use items.[1] The sanitary market size is predicted to increase by 3% until 2032 and reach 578 billion USD in 2032.[2,3] A representative example of extensively consumed sanitary items is single-use menstrual products, which today can contain up to 90 wt% of plastics, considering all the layers that assemble these (*i.e.*, plastic films, nonwovens, fluff pulps and the absorbent core layer).[3–6] An average woman during her reproductive lifespan uses approximately 11 000 single-use menstrual products,[2] which translates to approximately 25 kg of plastic waste per woman (taking 2.6 g as the weight of a typical daily pad). Further, the extended use of synthetic menstrual products has been revealed to expose the sensitive intimate tissue of individuals to toxic or carcinogenic chemicals, such as volatile organic compounds, phthalates, dioxins, and furans,[2,7] which are readily absorbed in the body.[8,9] In the last decade, some attempts have been made to promote the use of recyclable and/or polysaccharide-based foams as a more sustainable choice than traditional absorbent materials, as this core typically represents up to 50% of the total weight of a sanitary pad.[10,11] However, even if marked as recyclable/compostable, single-use sanitary pads are disposed of in landfills or incinerated due to their content of biological matter.[4,12] Therefore, it is crucial to focus on developing sustainable alternative layers that consider the choice of raw materials and their impact on the ecosystems, for instance, avoiding the risk of microplastics upon disposal.

[a]*Division of Polymeric Materials, Department of Fibre and Polymer Technology, KTH Royal Institute of Technology, Stockholm, SE-100 44, Sweden. E-mail: ajcv@kth.se; Tel: +46 70 166 7449*
[b]*Division of Industrial Biotechnology, Department of LIFE Sciences, Chalmers University of Technology, Gothenburg, SE-412 96, Sweden*

†Electronic supplementary information (ESI) available. See DOI: https://doi.org/10.1039/d4lp00323c

‡First shared authorship. The first authors contributed equally to this manuscript.

An interesting alternative to synthetic polymers used in absorbent layers reported in recent literature is biopolymers that possess good thermomechanical processability using continuous and environmentally friendly methods.[13–19] Within the realm of readily thermomechanical processed biopolymers, wheat-gluten protein (WG) is an attractive choice, being an abundant low-cost co-product from the starch industry.[19–21] Previous works have shown that bioplastics made out of gluten are readily biodegradable and do not release eco-toxic components or persistent microplastics into the environment.[13,22] The unique protein composition of WG (*i.e.*, gliadin and glutenin) is responsible for their exceptional viscoelastic behavior and the formation of stable 3D networks when thermomoulded, due to disulfide and hydrogen bonds that are formed.[18,23,24] Such thermomechanical properties give WG the possibility to be manufactured and shaped by applying established processing methods, such as extrusion, injection and compression moulding.[23,25–29] Recently, WG has been demonstrated as a suitable candidate for producing a porous structure with the addition of chemical blowing agents, such as sodium bicarbonate (SBC) and ammonium bicarbonate (ABC), with liquid uptake capacities promising for their use as single-use absorbents.[28,30–32] However, to our knowledge, the mechanical/structural characteristics of these materials simulating operating/service conditions relevant to single-use absorbent layers contained in sanitary items have not been assessed, which is of utmost importance for their further validation as biopolymeric alternatives in these applications.

In this study, we produced flexible porous absorbent pads (foams) from WG using oven expansion at low temperatures with a stable microstructure and high liquid absorption under load. The materials were foamed using sodium bicarbonate (SBC) and ammonium bicarbonate (ABC) as chemical blowing agents. The porosity and structural integrity of the absorbent pad layer were dependent on the choice of blowing agent and processing temperature. The elastic recovery of the materials also relied on the blowing agent used, and the properties matched that of highly porous synthetic absorbents used in commercial disposable sanitary pads. The study guides through relevant performance indicators of these gluten-absorbent pad layers during usage and addresses key needs to increase the competitiveness of these new readily processable porous proteins as alternatives to today's plastic absorbent materials. The possibility to contribute to studies producing fossil-free disposable sanitary products allows us to take the next step into increasing the reliability of these new types of plastic-free absorbent layers compared to traditionally used absorbents and even envision the design of other layers that are needed to assemble a complete disposable sanitary product.

2. Experimental

2.1 Materials

Wheat gluten powder (WG) was supplied by Lantmännen Reppe AB, Sweden. The powder consisted of 85 wt% wheat gluten protein (N × 6.25), 5.8 wt% wheat starch, 1.2 wt% lipids, 1 wt% ash, and 7 wt% water. Glycerol (ACS ≥98%), sodium bicarbonate (SBC, $NaHCO_3$, ACS ≥98%), and ammonium bicarbonate (ABC, NH_4HCO_3, ACS ≥98%) were purchased from Sigma-Aldrich, Sweden. *n*-Hexane (C_6H_{14}, ACS ≥98%) was purchased by VWR International, Sweden. The defibrinated sheep blood was purchased from Håtuna lab (Sweden). The water used was Mili-Q water (MQw, 18.2 MOhm cm at 25 °C).

2.2 Pad layer prototype preparation

The sample preparation process is shown in Fig. 1. In brief, 100 g of WG powder was homogenously mixed with 5 g of SBC or ABC (achieving 5 g of foaming agent per 100 g WG powder). Thereafter, 5 g of MQw and 50 g of glycerol per 100 g WG were added and mixed thoroughly to form the plasticized gluten formulation. 20 g of the WG mixture was placed into a steel mould with 2 mm thickness and pressed in between two steel plates covered with polytetrafluoroethylene (PTFE) sheets on both sides of the sample to prevent the material from sticking to the metal. The mixture was expanded in a Memmert UF 260 oven (Fan: 50% and Flap 100%) for 20 min at 70 and 120 °C for ABC and SBC, respectively. The actual recipes and the choice of processing route (oven expansion) were selected based on previous work showing that such processing route resulted in the highest porosity.[32] The pads were dried overnight at 40 °C in a ventilated oven and were then stored in a desiccator containing silica gel before any test. The full description of the samples is given in Table 1. The reference samples prepared only with glycerol are named WG/Gl, and the samples with SBC and ABC are referred to as WG/Gl-SBC and WG/Gl-ABC, respectively.

2.3 Density and porosity

The density was calculated using two methods. First, the foam's apparent density (ρ_a) was calculated by die-cutting three cylinders from random locations along the final product (Fig. 1d). Then, the weight of the dry samples in kg (w) was divided by their respective volume in m^3 (V). The dimensions of each sample were measured at three places with a digital caliper. The apparent density (ρ_a) is estimated according to eqn (1).

$$\rho_a = \frac{w}{V} \tag{1}$$

The porosity of the foams was estimated by eqn (2), using the density of solid WG material (1280 ± 20 kg m^{-3}) as a reference.[32]

$$\text{Porosity } (\%) = (1 - (\rho_a/1280)) \times 100 \tag{2}$$

The density was also estimated using a three-component model based on a modified Archimedes principle, described in eqn (3).[33]

$$\rho = w_a/V_{total} \tag{3}$$

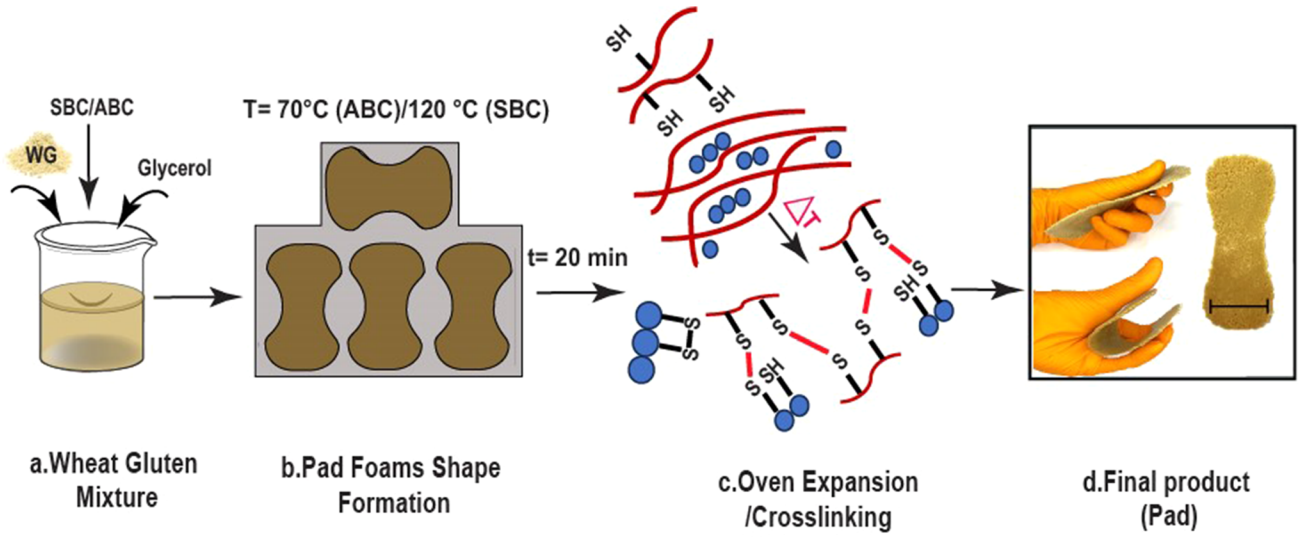

Fig. 1 Experimental protocol for the production of the protein pad layers, involving the mixing of the protein, glycerol and foaming agent (a), spreading the mixture in the moulds evenly for the oven expansion process (b), allowing for the formation of crosslinks between glutenin (represented by red chains containing –SH) and gliadin (represented by blue units containing –S–S–) in the protein matrix and foaming induced by the bicarbonates (c). The scale bar in the final pad (d) is 5 cm.

Table 1 Sample nomenclature and composition

Sample name	SBC (g per 100 g of protein)	ABC (g per 100 g of protein)	MQw (g per 100 g of protein)	$T_{processing}$ (°C)
WG/Gl-120	—	—	5	120
WG/Gl-SBC-120	5	—		
WG/Gl-70	—	—		70
WG/Gl-ABC-70	—	5		

All formulations include 50 g glycerol per 100 g of protein.

where w_a is the weight in the air and the total volume (V_{total}) is the sum of the volumes of open pores, closed pores, and the gluten/glycerol matrix, according to eqn (4).

$$V_{total} = V_{open\ pores} + V_{closed\ pores} + V_{WG/GI} \quad (4)$$

The volume of the solid gluten/glycerol matrix ($V_{WG/G}$) was determined from eqn (5) by measuring the sample's weight in the air (w_a) with a Mettler Toledo AL104 balance (Switzerland) equipped with an Archimedes accessory attached to the balance. The weight was divided by the determined density of the solid gluten/glycerol mixture ($\rho_{WG/GI}$ = 1280 kg m^{-3}).

$$V_{WG/GI} = \frac{w_a}{\rho_{WG/GI}} \quad (5)$$

The volumes of open and closed pores were estimated with eqn (6) and (7), using the weight of the sample in air (w_a), the weight of the sample immersed in *n*-hexane (w_i) (ρ_H = 661 kg m^{-3}), and the weight of the sample immediately after being removed from *n*-hexane (wet sample, W_w).

$$V_{open\ pores} = \frac{w_w - w_a}{\rho_{liq}} \quad (6)$$

$$V_{closed\ pores} = \frac{w_a - w_i}{\rho_{liq}} - V_{WG/GI} \quad (7)$$

From the ratio of these volumes, the total volume and the porosity of open and closed pores were calculated from eqn (4).

2.4 Scanning electron microscopy (SEM) and energy-dispersive X-ray spectroscopy (EDS)

The surface and cross-section microstructure of the samples were assessed in a Hitachi Tabletop SEM (TM-1000, Japan) at 10 kV. For the sample preparation, the specimen was cryo-fractured with liquid nitrogen and subsequently broken into pieces. These cryo-fractured pieces were placed onto an aluminum specimen holder using conductive carbon tape. To evaluate the sample's microstructure after 24 h saline-swelling and after absorption under load, the samples were frozen at –35 °C and lyophilized for 48 h. The microstructure of these systems was also evaluated in a Hitachi field emission scanning electron microscope (FE-SEM S-4800, Japan). A voltage of 3 kV and a current of 10 μA were used, and the pad foams were sputtered with platinum/palladium, forming a 1–2 nm conductive layer and using an Agar High-resolution Sputter Coater (model 208HR, Japan). The elemental map analysis was performed using an EDS sensor (Oxford Instrument) attached to the

FE-SEM, at 10 kV and a current of 20 μA. The average pore size was obtained from a minimum of 50 measurements from the SEM micrographs using the Image J® software.

2.5 Prototype liquid absorption performance

The free swelling/uptake capacity (FSC) was assessed according to the NWSP 240.0.R2 standard by first placing approximately 200 mg of dried sample (w_d) into an empty tea bag and then immersing it in a saline solution (0.9 wt% NaCl in MQw) or defibrinated sheep blood up to 30 min. The tea bag was hooked into a glass rod and placed into a beaker containing the solution. After the desired immersion time, the tea bag with the sample was lifted for 10 s and gently placed on paper tissue for another 10 s to remove excess liquid before being weighed again (w_i). The w_i values were calculated by removing the tea bag's wet weight. The FSC results were obtained following the eqn (8).

$$\mathrm{FSC}\left(\frac{g}{g}\right) = \frac{w_i - w_d}{w_d} \quad (8)$$

After the FSC test was completed, the tea bags with the material were centrifuged at 1230 rpm (250*g*) for 3 min, and the weight was subsequently recorded (w_c). The centrifugation retention capacity (CRC) values were calculated according to the NWSP 240.0.R2 standard. The FSC test yields the swelling capacity of the materials without any external force, while the CRC addresses the capacity of the material to hold the liquid at extreme conditions (here spinning at 1230 rpm).

$$\mathrm{CRC}\left(\frac{g}{g}\right) = \frac{w_c - w_d}{w_d} \quad (9)$$

The materials' capacity to absorb liquid under a constant load was determined using the Absorbance Under Load (AUL) test according to the NWSP 240.0.R2 standard (illustrated in Fig. 2a). Here, 0.90 g of dry pads (w_d) with dimensions 20 × 20 mm^2 were used. A polyurethane (PUR) foam extracted from a commercial product was used here as reference material but weighed 0.06 g to match the same dimensions as for the gluten pads. The sample with a weight w_A was placed in an outer cylinder (ϕ = 6 cm), having a plastic grid at the bottom. A second inner cylinder was placed on the top of the sample containing a standard weight (w = 500 g, ϕ = 6 cm), resulting in pressures ranging from 19 to 21 psi (0.13–0.14 MPa), depending on the sample dimensions. The test is performed to simulate the pressure on the material when a newborn is sitting on top. The entire set-up was placed on a Petri dish with a ceramic porous plate (160–250 μm porosity) and filter paper. 180 ml of saline solution (0.9 wt% NaCl in MQw) was added to the Petri dish, which is sufficient to reach the top of the ceramic plate and enable the liquid to come into contact with the sample through the plastic grid. The absorption process was performed for up to 1 h, whereafter the entire set-up containing

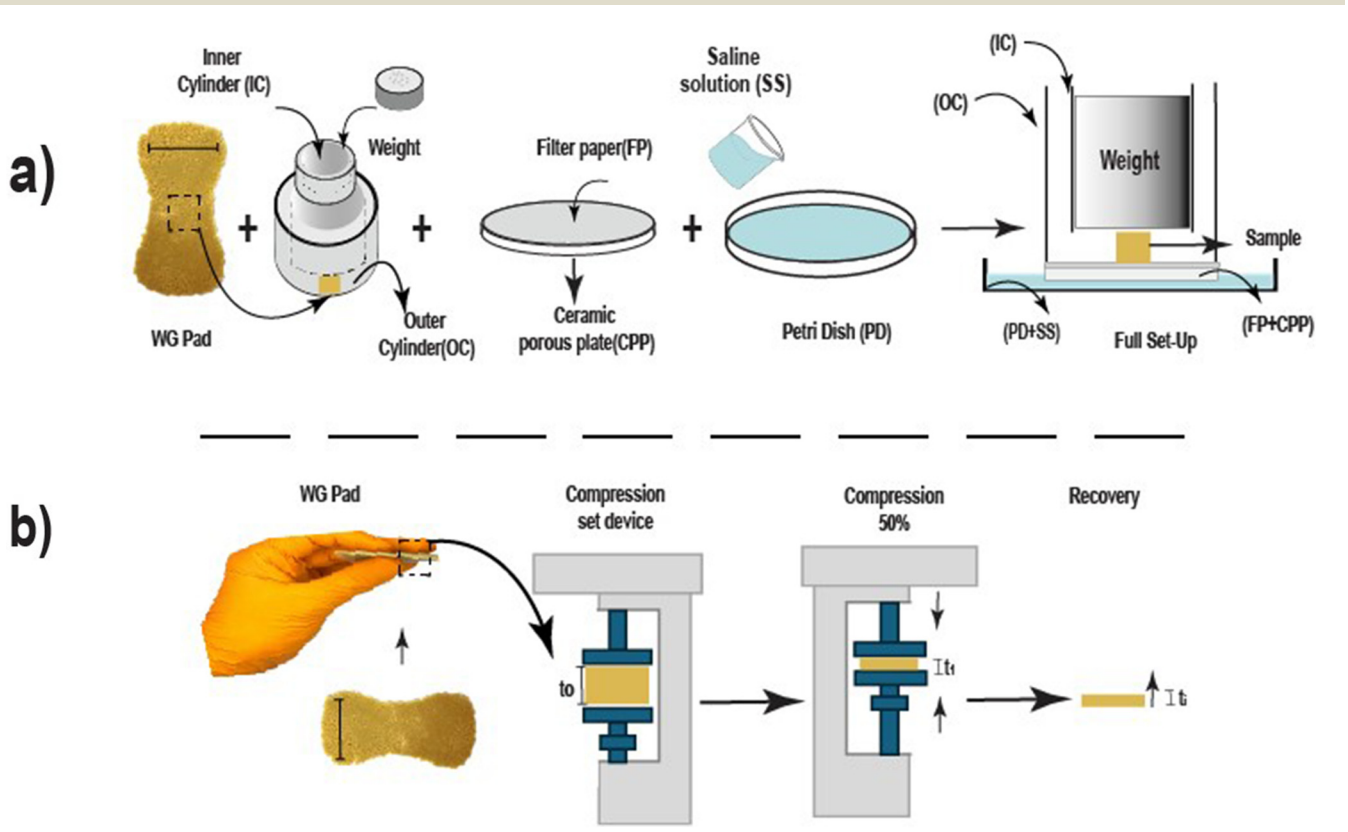

Fig. 2 Schematic illustration of (a) the Absorbance Under Load (AUL) set-up and (b) the Compression Set test. The scale bar in the WG pad layer is 5 cm.

the sample was removed from the Petri dish, and then the load was removed. The sample was weighed (w_B), and the AUL values were determined according to eqn (10). The experimental set-up is shown in Fig. 2a. FSC, CRC, and AUL are all standard tests to assess the product quality of new materials for their use in absorbent hygiene products.

$$\mathrm{AUL}\left(\frac{g}{g}\right) = \frac{w_B - w_A}{w_A} \quad (10)$$

2.6 Fourier-transform infrared spectroscopy (FTIR)

The infrared spectra were assessed to evaluate potential interactions between the WG foams, PUR pad layers and the water in the saline solution. 1 × 1 cm^2 pieces were cut and placed inside an oven at 45 °C for 48 h to remove the moisture, while for the wet samples, the pieces were placed in saline solution for 30 min. The FT-IR spectra were obtained with a Spectrum 100 equipment (PerkinElmer, USA). The scan resolution was 4.0 cm^{-1} with a scanning step of 1.0 cm^{-1}. The curve was obtained from 16 consecutive scans between 4000 and 600 cm^{-1}.

2.7 Mechanical properties

The compression set (CS) was determined to evaluate the potential permanent deformation of the foam pad layers at constant strain (Fig. 2b). This property is fundamental as the materials will be compressed during dry conditions if the user sits on the product. The test measurements were performed following the ASTM D395–18 standard and the samples conditioned at 23 ± 1 °C/50 ± 2% RH for 48 h. The compression set test consists of two plastic plates: one upper with a rectangular shape of 5 × 30 × 20 mm^3 and a lower circular plate of diameter 25 mm and 5 mm thickness. The pad foams were cut into 1 × 1 cm^2 squares and placed between the two plastic plates. The samples were then compressed to 50% strain for 0.5, 1, 3, and 24 h. After each compression, the samples were removed from the plates, and their height was measured after 0, 1, 5, 30, 60 min and 3 and 24 h to obtain the foam recovery as a function of time (t_i). The compression set (CS) was calculated according to eqn (11).

$$\mathrm{CS}\,(\%) = \frac{t_o - t_1}{t_o} \times 100 \quad (11)$$

where t_o is the 50% compressed sample thickness and t_1 is the final sample thickness.

The tensile testing of the WG-pad and PUR layers was performed using an Instron 5944 universal testing machine with a load cell of 500 N (Instron, USA). The extension rate was 10 mm min^{-1}, and five dumbbell-shaped specimens of each sample were tested. The stress–strain curve of each specimen was obtained, and the elastic modulus (E) was calculated from the slope of the linear region (below 5% strain). The stress at break (σ_b) and elongation at break (ε_b) were measured as the highest value of stress and the strain at the last recorded data point before the break, respectively. The dumbbell shapes used were die-cut at random places on the gluten and commercial PUR pads, and the conditioning followed the same procedure as described above for the compression set.

The tear propagation resistance of the WG-pad and PUR absorbent layers was determined with the same Instron 5944 universal testing machine and 500 N load cell for the tensile tests, following the ASTM D1938 standard. The samples were 75 mm long and 25 mm wide, and the thickness of the WG samples was between 2.5 mm for WG/Gl-ABC-70, 5.5 mm for WG/Gl-SBC-120, and 2.5 mm for the PUR foam. A notch of 50 mm in length was cut in the middle section of the samples. The tear deformation rate was 250 mm min^{-1}, and the distance between the grips was 50 mm. Three specimens of each sample were tested. The average tear propagation force was estimated from the resulting load-time curves. For the low-extensible samples (here, PUR), only the average tear propagation force was calculated by averaging the load over the extension range until the rupture of the sample. For the high-extensible samples (here, WG), the average tear propagation force was calculated together with the initial force to continue the propagation of the slit, the maximum force, and the extension at maximum force before the complete sample rupture.

2.8 Prototype bioactivity properties

The antioxidant activity of the WG-based pad layers was based on the assessment of scavenging activity against the DPPH radical (1,1-diphenyl-2-oicrylhydrazyl) following previously reported methodology with some adaptations for micro-assays.[34] The radical scavenging activity of the WG-based pad layers was quantified as the percentage of DPPH remaining in the solution after undergoing three cycles of oxidation to determine whether the antioxidant properties could be maintained over time.[35] Microplates were analyzed using the ClarioStar microplates reader (BMG Labtech, Germany), measuring absorbance at 517 nm. To determine the radical scavenging activity of individual additives employed in the production of WG-based pad layers, a 0.2 mM methanolic solution of DPPH was mixed with distinct concentrations of aqueous/methanolic additives solutions (ranging from 10 to 0.31 mg mL^{-1}). The result was expressed as EC50, indicating the concentration of antioxidants needed to reduce the initial DPPH concentration by 50%.

The antimicrobial activity was evaluated using a disk diffusion assay. Pathogenic bacteria, namely *Escherichia coli* (CCUG 10979) and *Bacillus cereus* (CCUG 7414), representing Gram-negative and Gram-positive bacteria, respectively, were employed. The *E. coli* strain was cultured in Tryptic Soy Broth (TSB) media, while the *B. cereus* strain was cultured in Lysogeny Broth (LB) media. The cell density concentration was adjusted to a McFarland scale of 0.5 using a spectrophotometer. In the disk diffusion test, 100 μL of the inoculated media was spread on the surface of solidified agar plates. Subsequently, the samples were placed onto the dried surface of the plates. The assessment of antimicrobial activity involved measuring the diameter of the antibacterial inhibition zone and observing bacterial growth on the contact surfaces of the material after an incubation period at 37 °C for 24 h.

2.9 Statistical analysis

Statistical analyses were performed with the least significant difference (LSD) in Fisher's procedure, evaluating the significance of the measurements ($p < 0.05$, 95% confidence level). These analyses were performed with the software Statgraphics 18 (USA). At least triplicates were used in each measurement.

3. Results and discussion

3.1. Prototype pad foam structure

Fig. 1 shows that the wheat gluten formulation (powder) was successfully processed into a porous material layer, resembling the structures of previously developed gluten-based porous materials.[28] The pad was successfully produced in the already-made shape shown in Fig. 1. Square samples of 15 × 15 cm^2 (Fig. S1†) were also produced to demonstrate that the final pad layer could be die-cut to the right shape as an alternative manufacturing route. The oven-expanded WG material resulted in flexible pad layers with rapid elastic recovery even after being folded several times, resembling the properties of commercial foams extracted from commercial sanitary pads (see Fig. 1d). The reference samples (manufactured without SBC or ABC) showed a low total porosity (~28%) and a density above 900 kg m^{-3} with also low pore sizes (Table 2 and Fig. 3a, c). These samples also had an open porosity of ~21%, according to Archimedes' density results. In contrast, the foam produced with SBC (*i.e.*, WG/Gl-SBC-120) displayed a highly porous microstructure (Fig. 3b), with the lowest apparent density and highest porosity (430 kg m^{-3} and 66%, respectively, see Table 2). This sample floated in the Archimedes test, impairing the estimation of its density and total porosity and suggesting the presence of a large content of closed pores.

All the samples were porous both in the interior and at the surface, which is relevant for absorbent material layers contained in sanitary products, allowing the liquid to penetrate efficiently (Fig. 3). The use of ABC resulted in larger pore sizes in the cross-section than those foamed with SBC. Further, the ABC sample had higher apparent and Archimedes densities than the SBC sample, including a wider pore size distribution. All in all, the results suggest that SBC is more suitable than ABC for manufacturing low-density foams with narrower pore size distributions when using "free expansion" oven foaming (Fig. S2d†). Based on the determined density, the SBC foam can be categorized as a high-density foam.[36,37] The presence of pores in the reference samples (*i.e.*, WG/Gl-120 and WG/Gl-70, Fig. 3a and c, respectively) has been previously explained as being due to rapid moisture uptake by the dry hygroscopic WG powder when removed from the desiccator just before the thermal processing (Fig. 1a). Furthermore, Fig. 3b–b.1 shows the presence of crystals of SBC or sodium carbonate (reaction products of the thermal decomposition of the SBC), as also observed in previous works.[23,25,28,33] In contrast, no crystals were observed in the sample with ABC (Fig. 3d and d1). Here, future work should focus on obtaining more regular and controlled porous structures so that they resemble further the structures of commercial absorbent foam pad layers used today in sanitary products, having up to 96% porosity.[38]

3.2. Functional absorption properties

Fig. 4a shows the free swelling capacity (FSC) in saline of the WG absorbent pad layers. The oven-expanded samples with SBC (WG/Gl-SBC-120) had the highest uptake among all samples produced, with *ca.* 3.5 g g^{-1} after 1 min and 4.5 g g^{-1} after 30 min. The reference pad layers and those with ABC experienced lower uptake, with a maximum of 1.5 g g^{-1} after 30 min. The high and rapid uptake for the SBC sample correlates well with its low density and high open porosity (Table 2), and are in line with previous work, where protein samples produced with SBC also had higher values than those produced with ABC.[28]

The capacity of the pads layers to retain saline solution was assessed by centrifuging the pads at 250*g* for 3 min after being swollen in saline for 30 min (CRC, Fig. 4b). WG/Gl-SBC-120 had the highest retention capacity, with *ca.* 0.7 g g^{-1}, followed by the sample with ABC (WG/Gl-ABC-70) with *ca.* 0.5 g g^{-1}. The samples that did not contain any foaming agent (WG/Gl-70 and WG/Gl-120) experienced the lowest CRC (0.4 g g^{-1}). The FSC and CRC values in saline solution for the WG-pad layers were 22% and 7% of the FSC and CRC values of commercial PUR foams in sanitary pads, which are also reported to have 96% porosity.[38] Previous works have shown that the degree of porosity and the pore architecture play a crucial role in increasing these values, as lyophilized gluten samples having 90% porosity reach the same absorption as the PUR foam layers. Thus, future work should focus on decreasing further the density of the material and increasing the porosity and pore interconnectivity while keeping the same upscalable processes reported here (oven expansion).

Table 2 Physical properties of the WG pad layers

Sample	Apparent density (kg m^{-3})	Porosity with apparent density (%)	Archimedes density (kg m^{-3})	Total porosity (%)	Open porosity (%)	Closed porosity (%)	Cross-section average pore size (μm)	Surface average pore size (μm)
WG/Gl-120	1039 ± 10^{c}	19 ± 1^{a}	919 ± 64^{a}	28 ± 5^{a}	21 ± 5^{a}	7 ± 0^{a}	147 ± 77^{a}	47 ± 34^{a}
WG/Gl-SBC-120	430 ± 16^{a}	66 ± 1^{c}	$<661^{a}$	—	—	—	342 ± 229^{a}	84 ± 60^{a}
WG/Gl-70	1017 ± 35^{bc}	21 ± 3^{ab}	928 ± 108^{a}	27 ± 8^{a}	21 ± 9^{a}	6 ± 1^{a}	171 ± 136^{a}	43 ± 17^{a}
WG/Gl-ABC-70	866 ± 125^{b}	32 ± 10^{b}	834 ± 64^{a}	35 ± 5^{a}	27 ± 4^{a}	8 ± 2^{a}	455 ± 476^{a}	212 ± 237^{a}

[a] The archimedes density of the WG/Gl-SBC-120 sample was not measured due to low density compared to the solvent used (ρ_{Hexane}: 661 kg m^{-3}). Different letters mean the values are significantly different ($P < 0.05$).

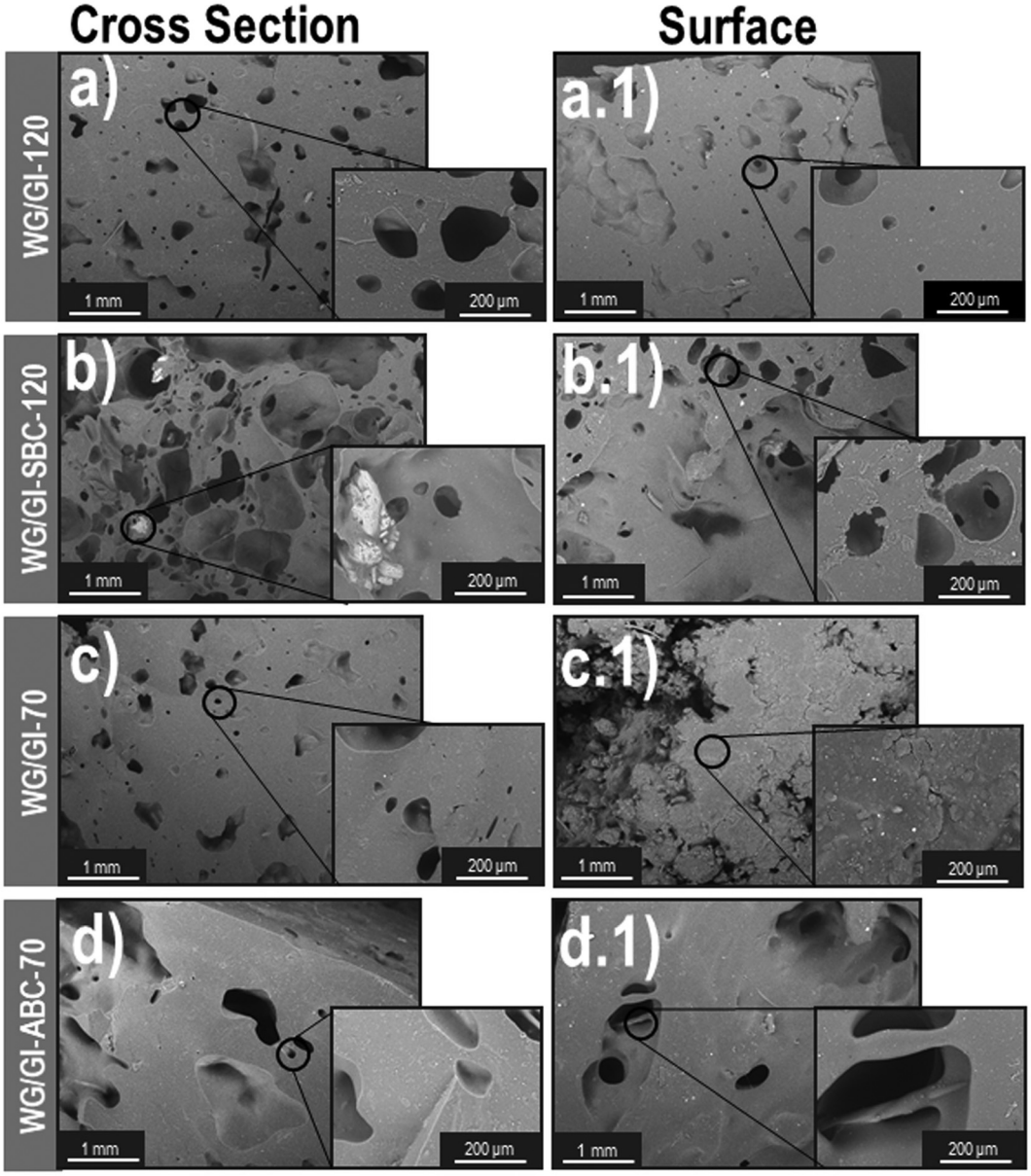

Fig. 3 Microstructure of the WG pad layers: The column (a–d) shows the cross-sections, and the column (a.1–d.1) shows the surface structure.

The blood uptake of the WG/Gl-SBC-120 sample was also the highest among the samples produced, with 1 g g^{-1} after 30 min, followed by WG/Gl-ABC-70 (Fig. 4c). The reference samples (WG/Gl-70 and WG/Gl-120) exhibited the same blood uptake values with a maximum uptake after 30 min (0.4 g g^{-1}). The blood uptake reported here was 4.4% of that of the PUR foam layer extracted from the commercial sanitary pads. The results indicate that the choice of processing temperature played a lower role (70 °C *versus* 120 °C) in increasing the blood absorption compared to the choice of the foaming agent (impacting considerably the microstructure of the materials). The lower absorption of the defibrinated blood compared to saline is due to its more complex composition and higher viscosity, containing a mixture of both polar and non-polar molecules.[28,39]

The WG/Gl-SBC-120 sample was swollen in saline for 30 min, freeze-dried, and cryo-fractured to assess if the saline solution uptake happened homogenously throughout the cross-section of the material (using EDS analysis). Fig. S3† displays the surface of the WG/Gl-SBC-120 after swelling and lyophilization. Fig. S4† shows a more porous structure after lyophilizing the swollen samples, ascribed to the water within the pore walls, forming ice crystals and sublimating during the lyophilization. Additionally, Fig. 4d shows the presence of Na and Cl ions on the sample surface and throughout the cross-section of the material after being exposed to the saline solution for 30 min. However, the content of Na and Cl was lower in the interior than in the surface region, indicating that the sample was not fully saturated with saline solution after the

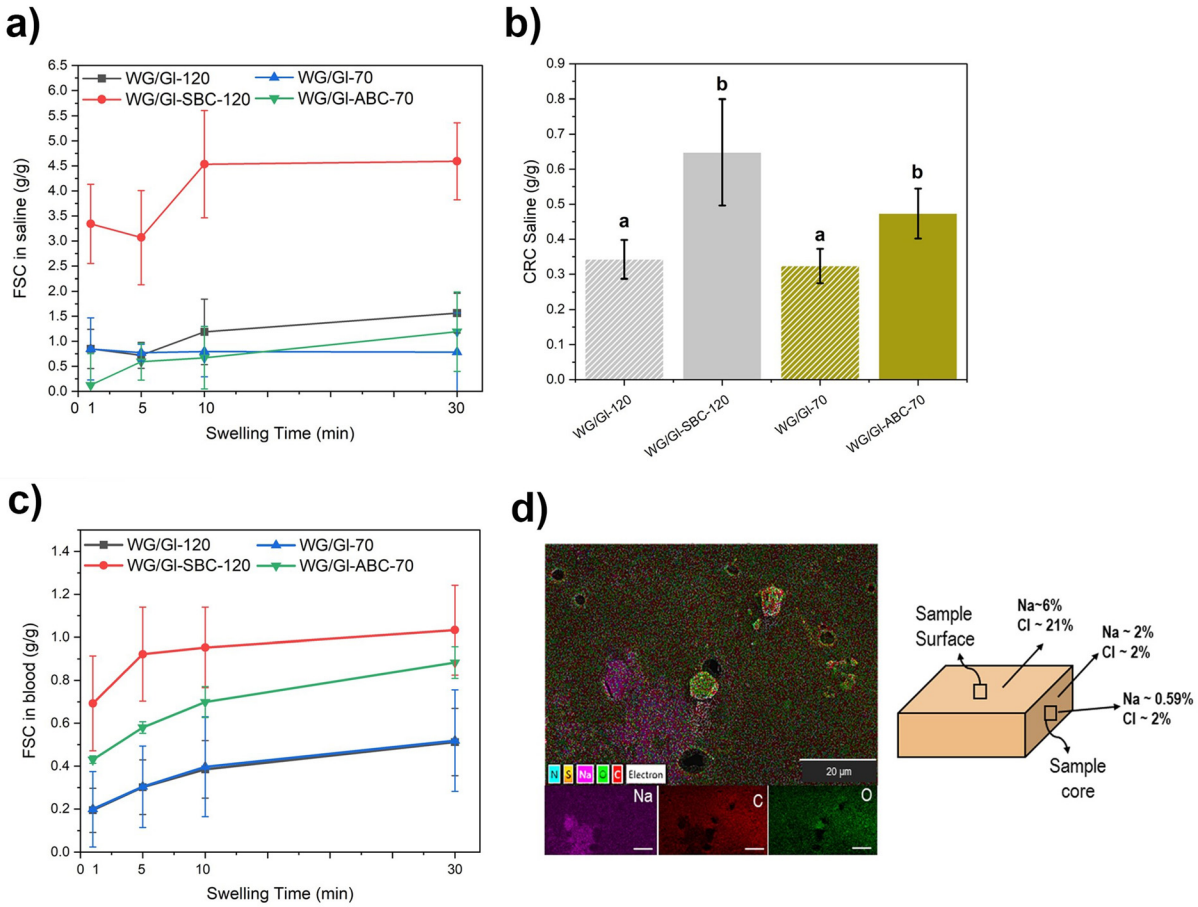

Fig. 4 Free swelling capacity in saline (FSC, a) and the centrifugation retention capacity after 30 min of saline swelling (CRC, b). (c) Free swelling capacity in defibrinated sheep blood. (d) Elemental analysis by EDS of the WG/Gl-SBC-120 cross-section. The scale bars in the inserts of *d* are 20 μm. Note: different letters mean the values are significantly different ($P < 0.05$).

30 min experiment. Alternatively, the reason could also be ascribed to the gluten matrix "sieving" the ions as the liquid penetrated the sample.

To validate the material as a future candidate in hygiene applications, an absorbance-under-load (AUL) test was performed as a representative assessment of the material mimicking operating conditions having a user on top. Fig. 5a shows the AUL values when using a piston, which results in a constant pressure of 0.20 psi (equal to 0.14 MPa) on the WG pad layers. The sample with SBC (WG/Gl-SBC-120) had the highest AUL value at 1.5 g g^{-1}, while the reference (WG/Gl-120) only showed an AUL of 0.65 g g^{-1}. The samples produced at 70 °C, with or without ABC, had an AUL value similar or slightly lower than the reference sample produced at 120 °C, despite that the actual pressure on these materials was slightly lower than on the SBC samples (Fig. 5b). The results show that the SBC-foamed sample maintained a high absorption despite being compressed, with an AUL value being half of the FSC value (compare Fig. 4a and 5a).

Fig. 5c–b.1 displays the WG/Gl-SBC-120 pad microstructure after the AUL test and lyophilization, showing that the microstructure was essentially unchanged despite the compression during the absorption test. On the contrary, the microstructure of the WG/Gl-ABC-70 sample contained collapsed pores (Fig. 5c, d and d.1). The reason for the ABC sample having a collapsed microstructure could be ascribed to the large pores being less efficient in keeping the structural integrity under constant load and the low foaming temperature resulting in less disulfide cross-linking in the gluten (*i.e.*, weaker pore walls).[23] The AUL values of the SBC sample were 25% of that of the commercial PUR foam from a menstruation pad used as a reference. The overall results from FSC, CRC, and AUL show the potential of protein-based foams as a replacement for today's synthetic foams in absorbent layers for sanitary pads while using readily scalable methods such as oven expansion. However, in order to increase the materials' competitiveness, future work should focus on decreasing the density of the materials and increasing further their FSC and AUL values. Also, to fully assemble an entire sanitary pad, future work should evaluate this material produced in different shapes and layers, such as non-wovens and fluff pulp and assess their breathability and tear/bursting properties.[40]

The potential interactions between the water in the saline solution (0.9 wt% NaCl) and the PUR and WG-pad absorbent

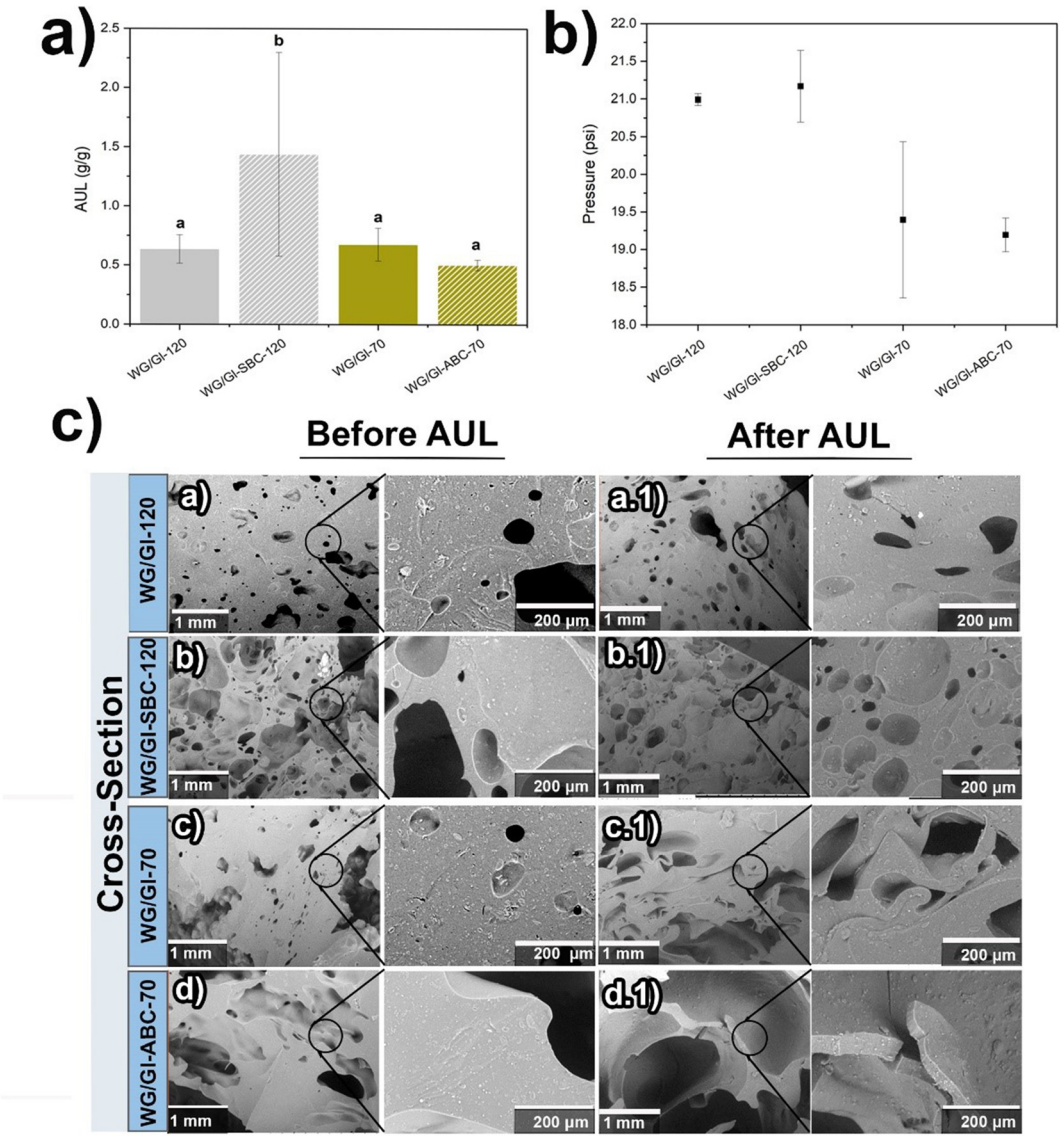

Fig. 5 (a) Absorption Under Load (AUL) of the WG pad layers and (b) the calculated pressure for each sample during the AUL test. (c) Cross-sectional microstructure of the lyophilized WG pad layers before and after AUL. Note: different letters mean the values are significantly different ($P < 0.05$).

layers were investigated with FTIR (Fig. S5†). All WG-based materials (dry and wet) had the characteristic amide I and II peaks at 1666 cm^{-1} and 1540 cm^{-1}, ascribed to the stretching vibration of C=O and deformation of N–H, respectively.[41] The PUR foam had characteristic peaks at 1200–1220 cm^{-1} (attributed to N–H bending) and 1705–1720 cm^{-1} (C=O bending), which originate from the urethane group.[42] The WG and PUR materials have bands peaking at different positions in the region above 3000 cm^{-1} (which originate from O–H and N–H stretch vibrations). In the presence of water, the resulting bands indicate contributions from the same peaks as well as from water (estimated peak position as a shoulder between 3250 and 3500 cm^{-1}). This indicates that water has not penetrated all parts of the samples. It also indicates that most of the water has the same degree of hydrogen bonding (a change in the degree of hydrogen bonding would shift the frequency of the O–H water band) in both the WG and PUR samples. Hence, this suggests that the portion of water that interacts directly with the material is small compared to the majority of the water present. It may also indicate that the interactions between water and the pad materials, including PUR, are similar.

Even though this work is focused on the use of the WG-based layers in sanitary pads, future work should also focus on revealing the detailed mechanism of water-protein interactions, in order to be able to increase the water absorbance further. Some suggested approaches to assess protein-water molecular interactions rely on atomic force microscopy (AFM), single-molecule force spectroscopy (SMFS), and modeling tools.[43]

3.3 Mechanical properties

Fig. 6 shows the compression set and strain recovery of the samples; relevant properties for the foam layer in a sanitary pad. Overall, the degree of recovery after a 50% compressive strain decreased with increasing compression time (from 30 min up to 24 h) for all foams (Fig. 6a–d). The SBC and ABC foamed samples showed, however, a high recovery (low compression set) of *ca.* 90 and 80%, respectively, after 30 min to 3 h compression (Fig. 6b and d). These specific periods of time were chosen based on established guidelines and recommendations for the use of sanitary pad products to maintain optimal menstrual hygiene and prevent health complications, *e.g.*, infections, bacterial growth or odors.[44,45] A high recovery was also observed for the samples without foaming agents at a shorter compression time. In general, the samples produced at 70 °C (WG/Gl-70 and WG/Gl-ABC-70) exhibited a lower 24 h-recovery after a short-term (30 min) compression. These results provide further evidence that the material's integrity is significantly influenced by the processing temperature, where the higher temperature results in greater disulfide cross-linking and more aggregated protein structures, leading to stronger pore walls.[46–49] The WG/Gl-SBC-120 pad layer exhibited the fastest recovery, which was comparable to the PUR material after 3 h recovery time (excluding the 24 h compression time, Fig. 6e). This superior recovery in the WG/Gl-SBC-120 pad is attributed to its homogenous porous structure, which enhances its ability to retain shape even after 24 h under compression, as well as its high porosity. Fig. 6f shows the compression set directly after removing the samples from the compression device and as a function of compression time. The result shows that the compression set is independent of the compression time and the type of sample. Further, the results are a first step in demonstrating the potential of new bio-polymeric sources (proteins) in replicating up to 97% of the elastic compression recovery set of synthetic absorbent layers used in sanitary pads.

Tensile test results show that the WG absorbent layers, irrespectively of the formulation and density, have higher elastic modulus (E) and larger extension at break (E = 3.2 MPa and ε_b = 225%) than the synthetic PUR absorbent layer, which makes them more competitive in terms of mechanical properties (Fig. 7a and b). The samples that showed the largest elongation at break were those processed at 70 °C (here WG/Gl-ABC-70 and WG/Gl-70), followed by WG/Gl-SBC-120, which was processed at 120 °C (see Fig. 7b). The increase in the extension at the break at lower temperatures can be ascribed to the aggregation/self-crosslinking temperature of gluten occurring at 90 °C[33] and the previously reported high alkalinity provided by SBC, inducing further crosslinking in the protein.[50]

The load-time time curves in the tear test of the WG-based and PUR layers are displayed in Fig. 7. The PUR showed a typical low-extensibility behaviour, with an average tear propa-

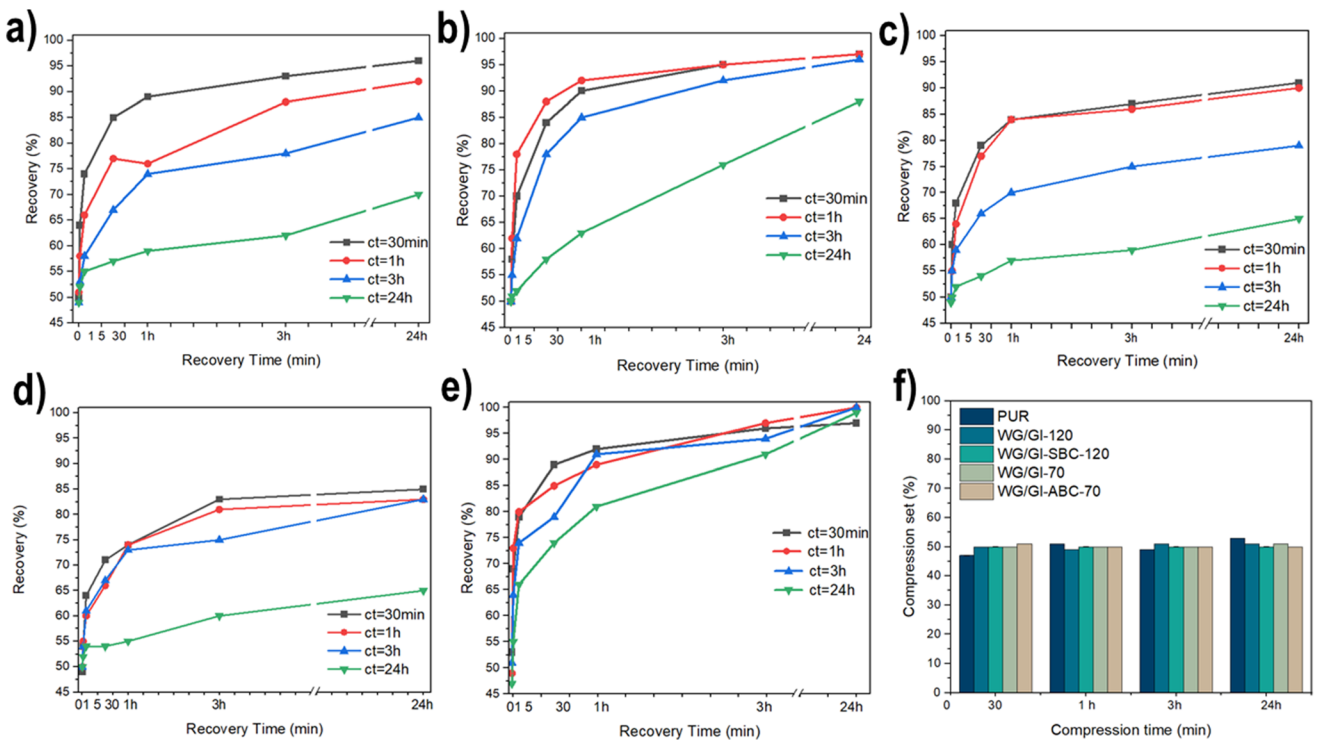

Fig. 6 Recovery of the samples as a function of recovery time after different periods of compression time: (a) WG/Gl-120, (b) WG/Gl-SBC-120, (c) WG/Gl-70, (d) WG/Gl-ABC-70, (e) PUR. (f) Compression set values directly after stress release (*ca.* 1 s). Note: the values are not significantly different (P < 0.05).

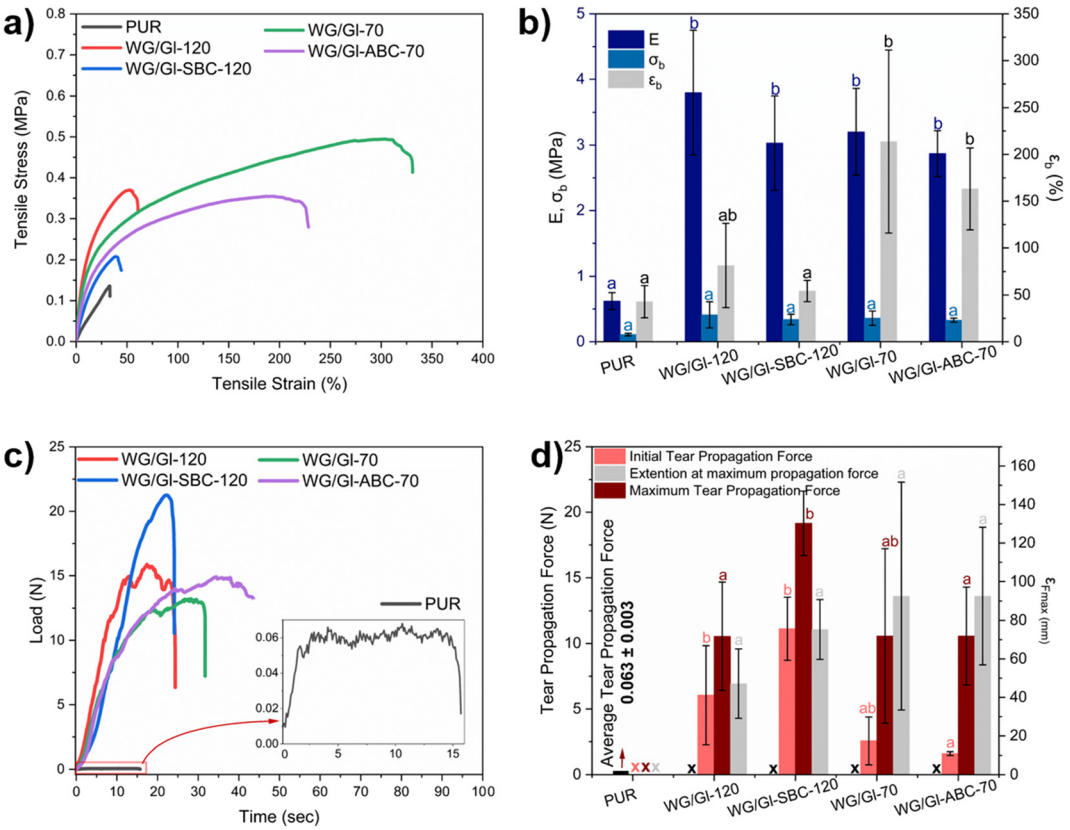

Fig. 7 (a) Tensile stress–strain curves of the WG pad and PUR layers and (b) average *E* (Young's Modulus), tensile stress at break (σ_b) and tensile elongation at break (ε_b). (c) Load-time charts for WG-based layers (highly extensible) and PUR (low extensible) and (d) average tear propagation force and maximum extension before total fracture. Note: the values (within the same color group) are not significantly different ($P < 0.05$).

gation force of 0.06 N, which is 300 times lower than those of the WG-pad materials. In addition, the WG-based materials showed a high extensibility behaviour during the tear test, with a high deformation visible around thecrack tip before its propagation (see ESI Video S1†). The result from the tear propagation test reveals that the WG materials have a higher resistance to tear propagation compared to PUR foams. The high resistance to tear propagation is an advantage for the future design of other layers needed to assemble a complete sanitary pad and future work should explore these properties together with measurables of the flexibility of these materials.

3.4 Antioxidant and antimicrobial properties

The antioxidant and antimicrobial activity of WG-based materials is shown in Fig. 8. These properties are important to determine for sanitary items since they provide input considering the risk of infections or odors during their use. Antioxidant activity helps to neutralize odor-causing oxidation reactions, while antimicrobial activity inhibits bacterial growth, ensuring better vaginal health and allowing for safer usage.[51] The samples produced at 120 °C were used in the test since the SBC pad layer had the best overall foam and absorption properties. The use of SBC as a foaming agent decreased the antioxidant activity by *ca.* 90% compared to the reference WG material. A hypothesis is that SBC is interfering in the rearrangement of disulfide (–S–S–)/sulfhydryl (–SH) groups at elevated temperatures, possibly lowering the amount of available sulfhydryl-groups, which, in turn, contributes to a decrease in the antioxidant activity of WG-pad materials containing SBC.[52]

The antimicrobial activity of WG-based materials, after 24 h and 37 °C incubation, was investigated, and the results are shown in Fig. 8b. The WG/Gl-120 and WG/Gl-SBC-120 materials presented surface antimicrobial activity against *E. coli* and *B. cereus*, as it can be seen by the non-opaque contact surface over the materials analyzed. This is particularly evident for WG/Gl-120 foams, which demonstrated more than 90% of the translucid surface, suggesting no microbial growth on the contact surface of the material for both bacterial strains evaluated. This can be explained by the potential contribution of the charged amino acid residues in WG, which contributes to antimicrobial activity due to lipophilicity, electronic properties, and electrical charges leading to interaction and degradation of bacterial cell morphology.[53] On the another hand, the incorporation of SBC to WB-based materials contributed to lowering the antimicrobial activity of the materials, as opaque regions are detected in the WG/G1-SBC-120 materials. This late result might be associated with

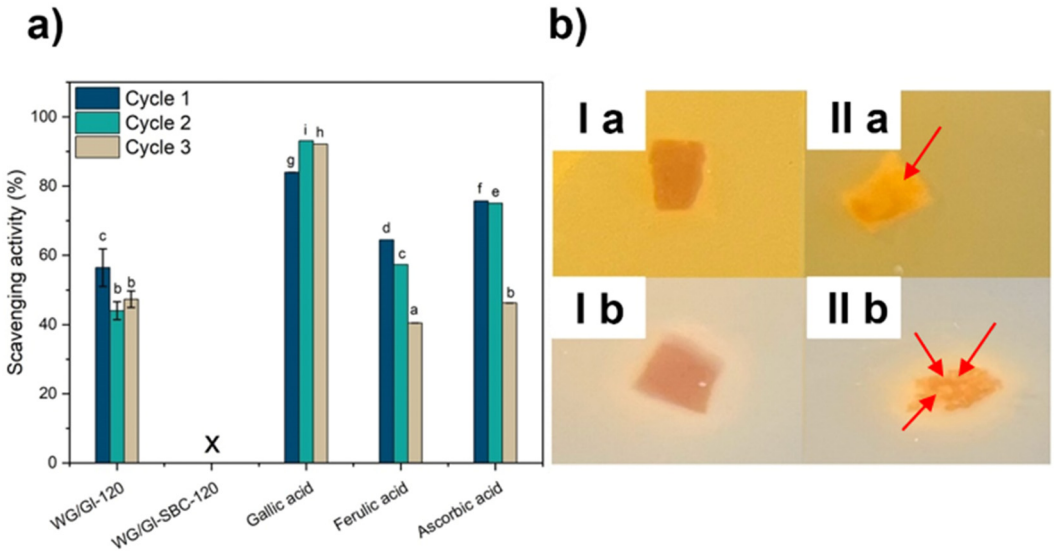

Fig. 8 (a) Antioxidant activity of the WG pad layers and representative species with known antioxidant properties, and (b) antibacterial activity of (I) WG/Gl-120 and (II) WG/Gl-SBC-120 materials against *E. coli* (a) and *B. cereus* (b), respectively. Note: *X* represents the sample in which no antioxidant activity was detected. Note: different letters mean the values are significantly different ($P < 0.05$).

the increase in the pore formation promoted by SBC as a blowing agent. This creates ideal conditions for bacterial growth, which can be correlated with the increase of contact surface and their capacity to adapt their metabolism.[54]

Both microorganisms are potential vaginal pathogens; *E. coli*, a Gram-negative bacteria, can cause infections through contamination from the gastrointestinal or urinary tract, while *B. cereus*, a Gram-positive spore-former, can infect the vagina through contact with contaminated surfaces. Both can lead to symptoms such as irritation, discharge, and discomfort, requiring prompt medical attention. Therefore, designing pads that reduce the risk of infections is of high importance.[55,56] Surface antimicrobial activity is interesting in cases where the prevention of microbial growth is required in touch with the material, such as wound healing, which demonstrates the potential of the developed pads to reduce/inhibit bacterial growth during the time it is used. It is worth mentioning that thermally processed gluten has previously been shown to have rapid biodegradation in soil and hydrolytic environments, which is relevant for developing absorbent layers in sanitary pads that rapidly degrade into safe molecules for the environment, avoiding risks for micro-plastic and PFAS accumulation.[28,50]

4. Conclusions

The fabrication of environmentally friendly WG (protein)-based absorbent layers displaying relevant properties to be considered as potential alternatives to synthetic foams contained in sanitary pad products, is reported. The use of gluten and non-toxic foaming agents enabled the fabrication of absorbent pad layers through simple batch expansion at low temperatures with a circular bioeconomy strategy. The produced protein pad layers showed high mechanical extensibility and superior tear resistance despite their low density (down to 430 kg m^{-3}), and the materials' microstructure was highly related to the bicarbonate type used. The results suggest that the absorption capacity (both with and without load) is primarily dependent on the blowing agent used, while the structural integrity of the materials depends on processing temperature. The processed pad layer using sodium bicarbonate resulted in AUL values up to 1.5 g g^{-1} after 1 h and with an almost complete shape recovery after 3 h of compression. Despite the incorporation of the blowing agent causing a decrease in the natural antioxidant activity of WG-based pads, the materials have exhibited antimicrobial activity against pathogen bacteria strains. The mechanical properties were within the range of reference PUR foams used in commercial absorbents, with relevant blood, saline uptake and mechanical properties making them competitive for absorbent layers in menstruation pads. The work paves an avenue towards including gluten-based alternatives in absorbent layers contained in sanitary pads, which reduces, on a global scale, the littering and landfilling and also limit microplastic issues, and opens up for future studies on manufacturing more layers that, when assembled form a full sanitary article.

Authorship contribution statement

Athanasios Latras: visualization, methodology, investigation, software, formal analysis, data curation, validation, writing – original draft, writing – review and editing. Mercedes A. Bettelli: visualization, methodology, investigation, software, formal analysis, data curation, validation, writing – original

draft, writing – review and editing. Pamela F. M. Pereira: methodology, validation, investigation, formal analysis, writing – original draft, writing – review and editing. Amparo Jiménez-Quero: investigation, resources, funding acquisition, formal analysis, validation, writing – original draft, writing – review and editing, supervision. Mikael S. Hedenqvist. resources, project administration, funding acquisition, formal analysis, validation, writing – review and editing, supervision. Antonio J. Capezza: conceptualisation, visualization, methodology, investigation, resources, project administration, funding acquisition, formal analysis, validation, writing – original draft, writing – review and editing, supervision.

Data availability

Data will be made available on request.

Conflicts of interest

The authors declare that they have no known competing financial interests or personal relationships that could have appeared to influence the work reported in this paper.

Acknowledgements

This work was financed by Formas (2019–00557, M. Bettelli; BioRESorb 2022–00362, A. J. Capezza). The authors, Pamela F. M. Pereira and Amparo Jiménez-Quero, acknowledge the European Union's Horizon Europe research and innovation program under the Marie Skłodowska-Curie grant agreement No 101107449 for funding supporting this work.

References

1 C. M. Galanakis, *Biobased Products and Industries*, Elsevier Science, 2020.
2 J. Marroquin, M. A. Kiomourtzoglou, A. Scranton and A. Z. Pollack, Chemicals in menstrual products: A systematic review, *BJOG*, 2023, 655–664.
3 V. Goel, P. Luthra, G. Kapur and S. Ramakumar, Biodegradable/Bio-plastics: Myths and Realities, *J. Polym. Environ.*, 2021, **29**, 1–26.
4 P. Notten, A. Gower and Y. Lewis, *Recommendations from Life Cycle Assessments*, United Nation Environ. Program., 2021, p. 2.
5 J. Ajmeri and C. J. Ajmeri, Nonwoven personal hygiene materials and products, *Appl. Nonwovens Tech. Text.*, 2010, 85–102.
6 A. Peter and K. Abhitha, Menstrual Cup: A replacement to sanitary pads for a plastic free periods, *Mater. Today: Proc.*, 2021, **47**, 5199–5202.
7 J. Moreno-Villafranca, V. M. Perez-Puyana, M. Jiménez-Rosado, M. Sabino and A. J. Capezza, Porous Thermoformed Protein Bioblends as Degradable Absorbent Alternatives in Sanitary Materials, *ACS Appl. Polym. Mater.*, 2023, **5**, 6989.
8 C. Sumpter and B. Torondel, A systematic review of the health and social effects of menstrual hygiene management, *PLoS One*, 2013, **8**(4), e62004.
9 Menstruating with dignity is a human right, **https://www.unfpa.org/menstrual-health**, (accessed 25 March 2024).
10 G. Reshma, C. R. Reshmi, N. Shantikumar and M. Deepthy, Superabsorbent sodium carboxymethyl cellulose membranes based on a new cross-linker combination for female sanitary napkin applications, *Carbohydr. Polym.*, 2020, **248**, 116763.
11 P. A. Mistry, M. N. Konar, S. Latha, U. Chadha, P. Bhardwaj and T. K. Eticha, Chitosan Superabsorbent Biopolymers in Sanitary and Hygiene Applications, *Int. J. Polym. Sci.*, 2023, **2023**, 4717905.
12 E. Peberdy, A. Jones and D. Green, A Study into Public Awareness of the Environmental Impact of Menstrual Products and Product Choice, *Sustainability*, 2019, **11**, 473.
13 S. Domenek, P. Feuilloley, J. Gratraud, M. H. Morel and S. Guilbert, Biodegradability of wheat gluten based bioplastics, *Chemosphere*, 2004, **54**, 551–559, DOI: **10.1016/S0045-6535(03)00760-4Get** rights and content.
14 R. Urade, N. Sato and M. Sugiyama, Gliadins from wheat grain: an overview, from primary structure to nanostructures of aggregates, *Biophys. Rev.*, 2018, **10**, 435–443.
15 W. S. Veraverbeke and J. A. Delcour, Wheat Protein Composition and Properties of Wheat Glutenin in Relation to Breadmaking Functionality, *Crit. Rev. Food Sci. Nutr.*, 2002, **42**, 179–208.
16 H. Wieser, P. Koehler and K. A. Scherf, Chemistry of wheat gluten proteins: Qualitative composition, *Cereal Chem.*, 2023, **100**, 23–35.
17 B. Lagrain, B. Goderis, K. Brijs and J. A. Delcour, Molecular basis of processing wheat gluten toward biobased materials, *Biomacromolecules*, 2010, **11**, 533–541.
18 C. J. R. Verbeek and L. E. Van Den Berg, Extrusion Processing and Properties of Protein-Based Thermoplastics, *Macromol. Mater. Eng.*, 2010, **295**, 10–21.
19 C. Wrigley, F. Bekes and W. Bushuk, in *Cereals & Grains Association*, Gliadin and Glutenin: The Unique Balance of Wheat Quality, 2006, pp. 3–32.
20 P. Shewry, Wheat grain proteins: Past, present, and future, *Cereal Chem.*, 2023, **100**, 9–22.
21 M. Zhang, R. Jia, M. Ma, T. Yang, Q. Sun and M. Li, Versatile wheat gluten: functional properties and application in the food-related industry, *Crit. Rev. Food Sci. Nutr.*, 2013, **63**(30), 10444–10460.
22 M. Jiménez-Rosado, M. Alonso-González, J. F. Rubio-Valle, V. Perez-Puyana and A. Romero, Biodegradable soy protein-based matrices for the controlled release of zinc in horticulture, *J. Appl. Polym. Sci.*, 2020, **137**, 49187.
23 M. A. Bettelli, A. J. Capezza, F. Nilsson, E. Johansson, R. T. Olsson and M. S. Hedenqvist, Sustainable Wheat

Protein Biofoams: Dry Upscalable Extrusion at Low Temperature, *Biomacromolecules*, 2022, **23**, 5116–5126.
24 Y. Yue, X. Liu, J. Wang, F. Jia, Q. Wang and X. Zhang, Change in physicochemical characteristics and molecular weight distribution of glutenin macropolymer induced by postharvest wheat maturation, *Qual. Assur. Saf. Crops Foods*, 2019, **11**, 789–798.
25 A. J. Capezza, E. Robert, M. Lundman, W. R. Newson, E. Johansson, M. S. Hedenqvist and R. T. Olsson, Extrusion of Porous Protein-Based Polymers and Their Liquid Absorption Characteristics, *Polymers*, 2020, **12**(459), 1–17.
26 A. J. Capezza, M. Lundman, R. T. Olsson, W. R. Newson, M. S. Hedenqvist and E. Johansson, Carboxylated Wheat Gluten Proteins: A Green Solution for Production of Sustainable Superabsorbent Materials, *Biomacromolecules*, 2020, **21**, 1709–1719.
27 S.-W. Cho, M. Gällstedt, E. Johansson and M. S. Hedenqvist, Injection-molded nanocomposites and materials based on wheat gluten., *Int. J. Biol. Macromol.*, 2011, **48**, 146–152.
28 M. A. Bettelli, E. Traissac, A. Latras, M. J. Rosado, A. Guerrero, R. T. Olsson, M. S. Hedenqvist and A. J. Capezza, Eco-friendly disposable porous absorbents from gluten proteins through diverse plastic processing techniques, *J. Cleaner Prod.*, 2024, **459**, 142419.
29 M. Gällstedt, A. Mattozzi, E. Johansson and M. S. Hedenqvist, Transport and tensile properties of compression-molded wheat gluten films, *Biomacromolecules*, 2004, **5**, 2020–2028.
30 T. C. Keener, G. C. Frazier and W. T. Davis, Thermal decomposition of sodium bicarbonate, *Chem. Eng. Commun.*, 1985, **33**, 93–105.
31 S. Mohan and P. Dinesha, Thermal dissociation kinetics of solid ammonium carbonate for use in NH3-SCR systems, *Chem. Pap.*, 2022, **76**, 6551–6556.
32 M. Jiménez-Rosado, L. S. Zarate-Ramírez, A. Romero, C. Bengoechea, P. Partal and A. Guerrero, Bioplastics based on wheat gluten processed by extrusion, *J. Cleaner Prod.*, 2019, **239**, 117994.
33 M. A. Bettelli, Q. Hu, A. J. Capezza, E. Johansson, R. T. Olsson and M. S. Hedenqvist, Effects of multi-functional additives during foam extrusion of wheat gluten materials, *Commun. Chem.*, 2024, **7**, 1–14.
34 W. Brand-Williams, M. E. Cuvelier and C. Berset, Use of a free radical method to evaluate antioxidant activity, *LWT-Food Sci. Technol.*, 1995, **28**, 25–30.
35 S. Baliyan, R. Mukherjee, A. Priyadarshini, A. Vibhuti, A. Gupta, R. P. Pandey and C. M. Chang, Determination of Antioxidants by DPPH Radical Scavenging Activity and Quantitative Phytochemical Analysis of Ficus religiosa, *Molecules*, 2022, **27**(4), 1326.
36 B. Alander, A. J. Capezza, Q. Wu, E. Johansson, R. T. Olsson and M. S. Hedenqvist, A facile way of making inexpensive rigid and soft protein biofoams with rapid liquid absorption, *Ind. Crops Prod.*, 2018, **119**, 41–48.
37 P. S. Liu and G. F. Chen, General Introduction to Porous Materials, *Porous Mater.*, 2014, 1–20.
38 C. E. Federico, Q. Wu, R. T. Olsson and A. J. Capezza, Three-dimensional (3D) morphological and liquid absorption assessment of sustainable biofoams absorbents using X-ray microtomography analysis, *Polym. Test.*, 2022, **116**, 107753.
39 T. Blomfeldt, R. Olsson, M. Menon, D. Plackett, E. Johansson and M. Hedenqvist, Novel Foams Based on Freeze-Dried Renewable Vital Wheat Gluten, *Macromol. Mater. Eng.*, 2010, **295**, 796–801.
40 2024.
41 C. G. Barreras-Urbina, M. Plascencia-Jatomea, F. J. Wong-Corral, M. Pérez-Tello, A. I. Ledesma-Osuna, J. A. Tapia-Hernández, D. D. Castro-Enríquez, E. O. Rueda-Puente and F. Rodríguez-Félix, Simple method to obtaining a prolonged-release system of urea based on wheat gluten: development and characterization, *Polym. Bull.*, 2020, **77**, 6525–6541.
42 Palm Kernel Oil Polyol-based Polyurethane as Shape Memory Material: Effect of Polyol Molar Ratio – Journal of Physical Science, **https://jps.usm.my/polyurethane-as-shape-memory-material/**, (accessed 7 December 2024).
43 Y. Shan, Y. Bao and S. Cui, Exploring water–macromolecule interactions at the single-molecule level: A comprehensive review, *Supramol. Mater.*, 2024, **3**, 100061.
44 Y. M. Demmu, G. M. Shifera, G. M. Ayana, D. Adare, B. Yazew, Y. T. Damtew and A. Geremew, Menstrual hygiene management and associated factors among adolescent school girls in gursum district, Eastern Ethiopia: Institution-based a cross-sectional study, *BMC Women's Health*, 2023, **23**, 1–7.
45 Understanding How Often Should You Change Your Pad?, **https://gladwellcare.com/pad-care-101-unraveling-the-science-of-timely-changes-for-healthy-incontinence/**, (accessed 6 July 2024).
46 H. Türe, M. Gällstedt, R. Kuktaite, E. Johansson and M. S. Hedenqvist, Protein network structure and properties of wheat gluten extrudates using a novel solvent-free approach with urea as a combined denaturant and plasticiser, *Soft Matter*, 2011, **7**, 9416–9423.
47 H. Ullsten, M. Gällstedt, E. Johansson, § Gräslund and M. Hedenqvist, Enlarged Processing Window of Plasticized Wheat Gluten Using Salicylic Acid, *Biomacromolecules*, 2006, **7**, 771–776.
48 Y. Ma, H. Zhang, D. Xu, Y. Jin and X. Xu, Wheat flour superheated steam treatment induced changes in molecular rearrangement and polymerization behavior of gluten, *Food Hydrocolloids*, 2021, **118**, 106769.
49 B. Lagrain, B. Thewissen, K. Brijs and J. Delcour, Mechanism of gliadin–glutenin cross-linking during hydrothermal treatment, *Food Chem.*, 2008, **107**, 753–760.
50 A. Jugé, J. Moreno-Villafranca, V. M. Perez-Puyana, M. Jiménez-Rosado, M. Sabino and A. J. Capezza, Porous Thermoformed Protein Bioblends as Degradable Absorbent Alternatives in Sanitary Materials, *ACS Appl. Polym. Mater.*, 2023, **5**, 6976–6989.

51 O. Sauperl, A. Zabret and L. Fras Zemljič, Development of advanced sanitary materials with the use of probiotic paste, *J. Eng. Fibers Fabr.*, 2020, **15**, 1–8.
52 S. Žilić, H. Akıllıoglu, A. Serpen, M. Barac and V. Gökmen, Effects of isolation, enzymatic hydrolysis, heating, hydratation and Maillard reaction on the antioxidant capacity of cereal and legume proteins, *Food Res. Int.*, 2012, **49**, 1–6.
53 S. Keyvani-Ghamsari, M. Rahimi and K. Khorsandi, An update on the potential mechanism of gallic acid as an antibacterial and anticancer agent, *Food Sci. Nutr.*, 2023, **11**, 5856–5872.
54 C. Jin and A. Sengupta, Microbes in porous environments: from active interactions to emergent feedback, *Biophys. Rev.*, 2024, **16**, 173–188.
55 D. E. O'Hanlon, T. R. Moench and R. A. Cone, In vaginal fluid, bacteria associated with bacterial vaginosis can be suppressed with lactic acid but not hydrogen peroxide, *BMC Infect. Dis.*, 2011, **11**, 200.
56 J. R. Brannon, T. L. Dunigan, C. J. Beebout, T. Ross, M. A. Wiebe, W. S. Reynolds and M. Hadjifrangiskou, Invasion of vaginal epithelial cells by uropathogenic Escherichia coli, *Nat. Commun.*, 2020, **11**, 1–11.